# Temporal and Spectral Correlations of Cyg X-1<sup>1</sup>

T.P. Li and Y.X. Feng High Energy Astrophysics Lab., Institute of High Energy Physics, Chinese Academy of Sciences, Beijing

L. Chen
Department of Astronomy, Beijing Normal University, Beijing

#### ABSTRACT

Temporal and spectral properties of X-ray rapid variability of Cyg X-1 are studied by an approach of correlation analysis in the time domain on different time scales. The correlation coefficients between the total intensity in 2–60 keV and the hardness ratio of 13–60 keV to 2–6 keV band on the time scale of  $\sim 1$  ms are always negative in all states. For soft states, the correlation coefficients are positive on all the time scales from  $\sim 0.01$  s to  $\sim 100$  s, which is significantly different with that for transition and low states. Temporal structures in high energy band are narrower than that in low energy band in quite a few cases. The delay of high energy photons relative to low energy ones in the X-ray variations has also been revealed by the correlation analysis. The implication of observed temporal and spectral characteristics to the production region and mechanism of Cyg X-1 X-ray variations is discussed.

Subject headings: accretion: accretion disk — stars: individual (Cygnus X-1) — X-rays: stars

#### 1. Introduction

Complex rapid fluctuation of the X-ray emission is a common characteristic of Galactic black-hole candidates and low-mass X-ray binaries (van der Klis 1995). X-ray variabilities on different time scales carry valuable informations about X-ray emitting regions. Cygnus X-1 is the brightest source in the hard X-ray sky and the most studied Galactic black hole candidate, its variability has been studied extensively. The Fourier transformation is a powerful tool in timing analysis and a lot of important results on Cyg X-1 variability, e.g., the shape of power spectral density, the coherence function and time delays between soft and hard light curve variability, are derived with this technique. Recently, with the Fourier analysis technique and observation data of the Proportional Counter Array (PCA) on board the Rossi X-ray Timing Explorer (RXTE), a series of studies for different states of Cyg X-1 have been done, e.g., studies of temporal properties of Cyg X-1 in the soft state (Cui et al. 1997a), during the spectral transitions (Cui et al. 1997b), and in the hard state (Nowak et al 1998). On the other hand, studying temporal properties of Cyg X-1 has been done with analysis techniques in the time domain, e.g., studying the shot-noise model by the autocorrelation function (ACF) of the light curves (Weisskopf, Kahn & Sutherland 1975, Sutherland, Weisskopf & Kahn 1978, Weisskopf et al. 1978, Priedhorsky et al. 1979), analysis of the cross-correlation function (CCF) between different energy bands (Priedhorsky et al. 1979, Nolan et al. 1981), modeling the light curve of Cyg X-1 by an autoregressive process (Pottschmidt et al. 1998). The frequency in a Fourier

<sup>&</sup>lt;sup>1</sup>To appear in The Astrophysical Journal

power spectrum or cross spectrum does not simply correspond to a certain time scale in the time domain which the physical process causing the variation really occurs in. Timing analyzing directly in the time domain is eventually necessary to study the variations on different time scales.

Temporal analyzing in the time domain usually requires the total amount of observed events and the signal to noise ratio of data much higher than that with the Fourier analysis. To overcome this difficulty, Negoro, Miyamoto and Kitamoto (1994) obtained average X-ray shot profiles from a Ginga observation of Cyg X-1 in the low state by superposing many shots through aligning their peaks and studied their properties. Recently we made analysis of the structures of X-ray shots with the characteristic time scale  $\sim 0.01-0.1$  s in the different states of Cyg X-1 with PCA/RXTE observations and an improved searching and superposing algorithm (Feng, Li & Chen 1998). From the obtained average shot profiles we have observed some interesting features, e.g., the average hardness of shot is lower than that of steady emission in the transition and hard states but higher than that in the soft state, the shot profile in the high energy band is narrower than that in the low energy band, etc. These observed phenomena give valuable hints on the shot production mechanism. In this work we study the correlation properties between the hardness and intensity and the energy dependence of temporal profiles on different time scales and for general variabilities, not only for shots in 0.01-0.1 s region.

As chaotic fluctuations of X-rays from Cyg X-1 are exhibited on wide time scales, from hours down to smaller than 1 ms, it is difficult to study the variation phenomena on a given time scale by simply using traditional analysis tools in the time domain, e.g., the correlation coefficient, autocorrelation function and cross-correlation function. Large time bin used in calculation will erase the information on shorter time scales. And the analysis result with a short time bin reflects not only the variation property on the short time scale, but is also affected by that on longer ones up to the total time period used in the calculation. In this work we make timing analysis of PCA/RXTE observations of Cyg X-1 by a modified approach in the time domain. For a given time bin  $\Delta t$ , we divide the total observation period into segments, each has a duration just several times of  $\Delta t$ , say  $10\Delta t$ . The correlation coefficient, ACF and CCF are calculated for each segment separately and the results are finally averaged. The resultant correlation coefficient, ACF and CCF, should be then related to the limited time scale region of  $\Delta t - 10\Delta t$ . In section 2 we present our analysis of correlation between hardness and intensity by this approach. The difference of ACF widths or time lag between low and high energy bands are usually much smaller than the time scale studied, which is another difficulty for timing analysis in the time domain. We try to use a technique similar to that in the vernier scale to measure the small difference in terms of a large time bin and present the results on energy dependence of temporal profiles of Cyg X-1 X-ray emission on different time scales in section 3. The implications of observed temporal and spectral characteristics to the production region and mechanism of Cyg X-1 X-ray variations are discussed in section 4.

### 2. Correlation between Hardness and Intensity

A series of observations of Cyg X-1 had been performed by RXTE in 1996. On 1996 May 10 (131 day of 1996) the All Sky Monitor on RXTE revealed the Cyg X-1 started a transition from the normal hard (low) state to the soft (high) state. After reaching the soft state, it stayed in this state for nearly 2 months before going back down to the hard state (Cui et al. 1997b). We use data of PCA/RXTE (2–60 keV) in 11 observational periods, including three periods during the hard-to-soft transition, three the soft state, two the soft-to-hard transition and three the hard state. The typical time duration of a period is, say,  $\sim 2000$  s. Two modes of PCA data are used in our analysis. One is the Event Mode with 16 energy

bands covering 13.1–60 keV with the time resolution of 16  $\mu$ s. The other is Single-Bit Mode including 2–6.5 keV and 6.5–13.1 keV bands (or 2–5 keV and 5–13.1 keV bands for the used data of hard states) with the time resolution of 125  $\mu$ s. The version 4.1 of standard RXTE ftools is used to extract the PCA data and version 1.5a of the background estimator program to estimate the background. The corrections of collimator response and barycentric time are applied to the chosen data of an observation period. The background-subtracted light curves of the low energy band  $f_1$  (2–6.5keV) (or 2–5 keV for the hard state), middle energy band  $f_2$  (6.5–13.1keV) and high energy band  $f_3$  (13.1–60keV) with a selected time bin  $\Delta t$  can be obtained by rebinning and making background correction for each energy band respectively. From the three light curves we derive the profiles of intensity f(2–60keV) and hardness ratio  $h = f_3/f_1$  and use the correlation analysis to study the relationship between the X-ray intensity and hardness ratio. The correlation coefficient for n pairs of h, f values is defined as

$$r(h,f) = \sum_{i=1}^{n} (h(i) - \overline{h})(f(i) - \overline{f}) / \sqrt{\sum_{i=1}^{n} (h(i) - \overline{h})^2 \sum_{i=1}^{n} (f(i) - \overline{f})^2}$$
 (1)

For a given time bin  $\Delta t$  the studied observation period is divided into total N segments with a duration of  $10\Delta t$  each. In our analysis, a data bin is defined as an effective one if the total length of data gaps in the bin is less than  $0.1\Delta t$ , and just such segments are used in which the number of effective bins  $n\geq 8$ . We calculate the correlation coefficients r(i) of each segment  $i,\ i=1,2,...,N,$  by using Eq.(1), and then their average  $\overline{r}=\sum_{i=1}^N r(i)/N$  and standard deviation  $\sigma(\overline{r})=\sqrt{\sum_{i=1}^N (r(i)-\overline{r})^2/N(N-1)}$  for the period. Table 1, 2 and Figure 1 show the obtained averages of correlation coefficients between h and f(2--60keV) and their standard deviations for the 11 periods with time bin (time scale) 1 ms, 10 ms, 0.1 s, 1 s, 10 s, 20 s and 50 s respectively, where the hardness ration h is determined by the two energy bands of 2–6.5 keV and 13.1–60 keV for the periods of soft and transition states and 2–5 keV and 13.1–60 keV for the hard states. The lower band range of Single-Bit mode of PCA observations for the hard state of Cyg X-1 in 1996 is a litter bit different with that of public observations for the soft and transition states, this difference will not considerably change the results in this work.

Figure 2 (a)–(d) show the light curves and hardness ratio profiles in 50 s time bin and their trends smoothed by the least-square fitting for four example periods in different states. Comparing the light curves (fluctuated solid curves) and the corresponding hardness ratio profiles (fluctuated dotted curves) in the four periods in different states, one can see that a near perfect correlation between the hardness and intensity is shown in the upper right-hand panel of Fig.2 for the soft state, but rather complex feature, a mixture of positive and negative correlations, for other states.

The plots of correlation coefficient versus time scale for different states are shown in Figure 3. The value of correlation coefficient r(h,f) in Fig.3 on a time scale and for a given state is the weighted average of  $\overline{r}(k)$  from k=1,...,M considered periods in this state, i.e.,  $<\overline{r}>=\sum_{k=1}^M\omega(k)\overline{r}(k)/\sum_{k=1}^M\omega(k)$ ,  $\omega(k)=1/\sigma^2(\overline{r}(k))$ ; its error is determined by both the errors of each  $\overline{r}$  values and their dispersion, i.e.  $\sigma=\sqrt{\sigma_1^2+\sigma_2^2},\ \sigma_1^2=1/\sum_{k=1}^M\omega(k),\ \sigma_2^2=\sum_{k=1}^M(\overline{r}(k)-<\overline{r}>)^2/(M-1).$ 

Some interesting features of state dependence of correlation coefficient r(h, f) can be seen from Tables 1, 2 and Figures 1–3. On the shortest time scale ( $\Delta t = 1$  ms) anti-correlations are always found in all observation periods. On the longer time scales (0.01–50 s) the correlation property when Cyg X-1 in soft states is quite different with what in transition and hard states. For soft states, positive correlations between the hardness ratio h and intensity f exist on all time scales between 0.01 s and 50 s. The correlation coefficients r(h, f) increase monotonically and reach to near unity along with the time scale increasing

from 0.01 s to 50 s. On the other hand, the correlation coefficients are negative or near zero when Cyg X-1 is in transition or hard states. The error bars in Tables 1, 2 and Figures 1, 3 are derived from the standard deviations of the obtained correlation coefficients of all available segments. As the total number of correlation coefficients is always large for any state and time scale studied, their deviation can give a reasonable estimate of the statistical uncertainty in the derived average value. The increasing trend of the correlation coefficients with the time scale in the soft state and the difference between the correlation in the soft state and that in the other states are statistically significant.

#### 3. Energy Dependence of Temporal Profiles

The Fourier frequency-dependent time delays of high-energy photons relative to low-energy ones in the X-ray variations of Cyg X-1 have been observed for some time and are attracting an increasing amount of attention to using it as a diagnostic of the emission mechanism and emitting region (e.g., Kazanas, Hua & Titarchuk 1997, Hua, Kazanas & Titarchuk 1997, Böttcher & Liang 1998b, Nowak et al 1999). Recently, from analyzing many X-ray shots of Cyg X-1 in different states we confirm the existence of time delays of hard photons behind soft photons in a shot (Feng, Li & Chen 1998). A notable finding from our shot analysis is that the shot profile in the high energy band is narrower than that in the low energy band, which is not consistent with the prediction of the simple Comptonization models. It is important to study the energy dependence of temporal profiles of Cyg X-1 in different states and on different time scales directly in the time domain.

We take a procedure similar to that used in section 2 to derive the average width of the autocorrelation functions and study the temporal correlation of two light curves in different energy bands on different time scales. For a given time scale  $\Delta t$ , the observation period studied is also divided into segments with a duration of  $10\Delta t$  each. The autocorrelation function of the zero-mean time series  $v(i) = f(i) - \overline{f}$  of a segment is usually defined as

$$ACF(k) = \sum_{i} v(i)v(i+k)/\sigma^{2}(v) \quad (k=0,\pm 1,...)$$
 (2)

where  $\sigma^2(v) = \sum_i (v(i))^2$ , f(i) is the average intensity in the time bin  $(i-1)\Delta t - i\Delta t$ . The cross-correlation function of two series  $v_l$  and  $v_m$  corresponding to two energy bands is usually defined as

$$CCF_{l,m}(k) = \sum_{i} v_l(i)v_m(i+k)/\sigma(v_l)\sigma(v_m) \qquad (k=0,\pm 1,...)$$
 (3)

The corresponding time lag of ACF(k) or CCF(k) is  $\tau = k\Delta t$ . With the ACF and CCF defined above, it is difficult to measure time lags  $\tau \leq \Delta t$ . To get necessary resolution for time lags we modify the above definition of ACF and CCF that we can use a time bin  $\delta t < \Delta t$  for time lag. For the convenience we use the time instead of the bin number as the argument in the expression of ACF and CCF: use  $ACF(\tau)$  and  $CCF(\tau)$  to represent the values of ACF and CCF at the time lag  $\tau$ , f(t) the average intensity in the time duration  $t - t + \Delta t$  and  $v(t) = f(t) - \overline{f}$ . We define the autocorrelation function of the light-curve f

$$ACF(\tau) = \sum_{i} v(i\Delta t)v(i\Delta t + \tau)/\sigma^{2}(v)$$
(4)

and the cross-correlation function between two light-curves  $f_l$  and  $f_m$ 

$$CCF_{l,m}(\tau) = \sum_{i} v_l(i\Delta t) v_m(i\Delta t + \tau) / \sigma(v_l) \sigma(v_m)$$
(5)

With the ACF and CCF at  $\tau = k\delta t, k = 0, \pm 1, ...$ , we can study temporal variations on the time scale of  $\Delta t - 10\Delta t$  with a necessary time resolution  $\delta t$ . For a studied observation and a given time bin  $\Delta t$ , the total observation period is divided into N segments with a duration of  $10\Delta t$  each. For a segment j we calculate the autocorrelation function of the light curve in the low energy band,  $ACF_1$ , and that in the high energy band,  $ACF_3$ , with the time lag bin  $\delta t$  of 1 ms from Eq.(4), and also  $CCF_{1,3}$  between the two bands from Eg.(5). We then find out the full width at half maximum,  $W_1(j)$ , from the profile  $ACF_1$ ,  $W_3(j)$  from  $ACF_3$ , and the time delay  $\lambda(j)$  of the high energy band relative to the low energy band. The time delay is determined by the maximum of the function  $CCF_{1,3}(\tau)/CCF_{1,3}(\tau=0)$ . The N segments are divided into M=10 groups with the segment numbers n(k) in each group k (k=1,2,...,M) being nearly equal to each other and  $\sum_{k=1}^{M} n(k) = N$ . The average of a concerned quantity x (x can be  $W_1, W_3$  or  $\lambda$ ) and its standard deviation for each group k can be calculated by using the following formulas

$$\overline{x}(k) = \sum_{j=1}^{n(k)} x(j)/n(k), \qquad \sigma(\overline{x}(k)) = \sqrt{\frac{\sum_{j=1}^{n(k)} (x(j) - \overline{x}(k))^2}{n(k)(n(k) - 1)}}$$
(6)

Finally we report the result for the observation as

$$x = \langle x \rangle \pm \sigma_1(x) \pm \sigma_2(x) \tag{7}$$

where

$$\langle x \rangle = \sum_{k=1}^{M} \omega(k) \overline{x}(k) / \sum_{k=1}^{M} \omega(k), \qquad \omega(k) = 1/\sigma^{2}(\overline{x}(k))$$

$$\sigma_{1}(x) = \sqrt{1/\sum_{k=1}^{M} \omega(k)}, \qquad \sigma_{2}(x) = \sqrt{\sum_{k=1}^{M} (\overline{x}(k) - \langle x \rangle)^{2} / M(M-1)}$$
(8)

The first error term  $\sigma_1(x)$  in the expression (7) represents the precision of  $\langle x \rangle$  as an average for the observation period, the second one  $\sigma_2(x)$  describes the dispersion of the M averages  $\overline{x}(k)$  within the observation.

We apply the formulas (6) – (8) to calculate the average ACF widths  $FWHM_1 = \langle W_1 \rangle$  in the low energy band,  $FWHM_3 = \langle W_3 \rangle$  in the high energy band, and the average time delay  $\langle \lambda \rangle$  between the two bands for six observations and show the results in Table 3 – 5. From Table 4 and 5 one can see that for all studied observations the temporal variations in the high energy band are always delayed relative to the low energy band on all time scales, and that on the time scale  $\Delta t = 0.1$  s the width of ACF in the high energy band is generally narrower than that in the low energy band. For an example, Figure 4 shows the average autocorrelation and cross-correlation functions of the low and high energy light-curves with the time bin  $\Delta t = 0.1$  s for the observation started at 143.7 day of 1996 when Cyg X-1 in the transition from hard state to soft state. The total duration of the observation is about 2230 s. The total effective bins of 0.1 s are divided into M=10 groups, each group has about n=208 segments of 1 s. For the 10 groups, the ACFwidth ratios,  $W_3/W_1$ , are all smaller than unity, they are  $0.797 \pm 0.029, 0.755 \pm 0.030, 0.746 \pm 0.031, 0.775 \pm 0.030, 0.746 \pm 0.030, 0.$  $0.033, 0.725 \pm 0.030, 0.715 \pm 0.029, 0.752 \pm 0.027, 0.749 \pm 0.030, 0.739 \pm 0.028$  and  $0.712 \pm 0.030$ . From the above values we finally obtain  $FWHM_3/FWHM_1 = 0.747 \pm 0.009 \pm 0.016$ . The above results show that the width of ACF in the high energy band being narrower than that in the low energy band is statistically significant for the observation. To compare our results on hard X-ray delay with that from Fourier spectral analysis, we plot the time lags as a function of  $1/\Delta t$  for four observations in Figure 5 (a)-(d). The time lags vs.  $1/\Delta t$  shown in Fig.5 are similar with the time lags vs. Fourier frequency obtained by Fourier spectral analysis (Cui et al. 1997b, Fig.8; Nowak et al 1998, Fig.10).

## 4. Discussion

There exists an obvious anti-correlation between the 2-60 keV intensity and spectral hardness of X-rays from Cyg X-1 in its long-term variability exhibited by its state transition between low/hard and high/soft states. One can find from Fig.2 that for the soft state the typical intensity is  $\sim 15$  cts/ms and hardness ratio between the high and low energy bands  $\leq 0.1$ , and for the hard state they are  $\sim 6$  and  $\geq 0.6$ , respectively. For shorter time scales, our analysis results show different correlation features in different states.

In a previous paper (Feng. Li & Chen 1998) we studied the spectral properties of average shots of Cyg X-1 on the time scale of about 0.1 s in soft, hard and transition states and found that the hardness during a shot is higher than that of the steady component around the shot in soft states but lower in transition and hard states. Fig.6(a) - Fig.6(d) show the intensity and hardness ratio profiles of average shots in the different states of Cyg X-1, where the average shots were obtained by using the same data as that presented in this paper. We can see from Fig.6(b) that for the soft state the hardness ratio peaks while the flux of the shot peaks, showing a positive correlation between the hardness and intensity. For the hard state, although the average hardness of the shot is lower than that of the steady emission, but there exist both positive and negative peaks during the shot, as shown in Fig.6(d), the net correlation for the shot should be quite small. For both the hard to soft transition state and the soft to hard transition state, the hardness variation during the shot is dominated by a negative peak, as shown in Fig.6(a) and Fig.6(c), the correlation coefficient should be negative. In fact we can calculate the correlation coefficient between the profiles of flux and hardness ratio of a shot. The derived r(h, f) for shots in Fig.6 within the range of  $\pm 0.2$ s around the shot peak are  $-0.44 \pm 0.14$  for the hard to soft transition state,  $0.89 \pm 0.07$  for the soft state,  $-0.38 \pm 0.15$  for the soft to hard transition state, and  $-0.04 \pm 0.16$  for the hard state, respectively. The state dependence of shot r(h, f) is generally consistent with what is shown in Table 1 and Fig.3 for the time scale of 0.1 s, except a considerable difference in quantity for the soft state. The shot of the soft state shows a nearly perfect correlation between the hardness ratio and flux, but the correlation coefficients for the soft state on 0.1 s time scale in Table 1 and Fig.3 are just about 0.3. As the correlation analysis in this paper is made for the temporal variability on a certain time scale in general, not only for shots, the obtained correlation coefficient being smaller than that of shots reflects the existence of other uncorrelated variation components, including noise. For the hard and transition states, the consistency between the results from our general correlation analysis on the 0.1 s time scale and those for shots indicates the variable flux on the 0.1 s time scale being dominated by shots. The trend of the correlation coefficients r(h, f) increasing monotonically and reaching to near unity along with the time scale from 0.01 s to 50 s may indicate the effect of uncorrelated noise being weakened on larger time scales.

The most remarkable result from our analysis is the state dependence of correlation features on the time scales of  $\sim 0.01~\rm s-\sim 50~\rm s$ . The correlation coefficients r(h,f) are always positive during soft states but negative or near zero during transition and hard states. It is widely believed that hard X-rays of Cyg X-1 come from inverse Compton scattering of low energy seed photons by high energy electrons in an accretion disk corona (ADC) (e.g., Eardley, Lightman & Shapiro 1975, Poutanen & Svensson 1996, Dove et al. 1997) or hot advection-dominated accretion flow (ADAF) (e.g., Esin et al. 1998). The steady or slowly varied component of the observed hard X-rays should be a global average of emission from different regions of the hot corona (ADC or ADAF), whereas a rapid variation can be produced at a local region where a disturbance occurs. The innermost region of the cold disk jointed with the hot corona is most probably a turbulent region where violent disturbances frequently take place and produce rapid varying low energy photons, causing variable X-ray emission through Comptonization in the nearby region of the hot corona. The difference between the hardness ratios of the rapid varied component and steady component may be

caused by a difference between the local temperature of the Comptonizing region to produce the rapid varied emission and the average temperature of the total corona.

Two different geometries in the ADC or ADAF model exist. One is the sphere+disk geometry: a spherical corona around the centric compact object with exterior accretion disk. And another is the slab geometry: the Comptonizing medium being a slab surrounding the disk. The predicted spectrum of Comptonization models with the sphere+disk geometry (Dove et al. 1997, Esin et al. 1998) can describe the observed X-ray spectrum of Cyg X-1 in the hard and transition states. The spherical corona exists only for accretion rates below some critical value. For the soft state, the disk extends down to the last stable orbit and the hot flow is restricted to the corona surrounding the disk (Esin et al. 1998). The temperature  $T_d$  of the disk is a function of radius: inner part has higher temperature (Frank, King & Raine 1992, Dove et al. 1997). The temperature  $T_c$  of corona embedding the cold disk is related to the disk temperature  $T_d$ : for the same value of the optical depth of the corona, the spectra of Comptonized photons are harder in the case of higher  $T_d$  (Haardt & Maraschi 1993, Dove, Wilms & Begelman 1997). Accordingly in the soft state with the slab geometry, the spectra of shots from the coronal region surrounding the innermost disk should be harder. On the other hand, for the transition and hard states the radial dependence of the coronal temperature in the central corona expected for an advection dominated accretion flow can be approximately represented as  $T_c \propto r^{-1}$  with r being the distance from the center of the black hole (Narayan & Yi 1994, Narayan, Mahadevan & Quataert 1998). The innermost orbit of the disk in the case of the sphere+disk geometry is located outside the spherical corona and its neighboring Comptonizing region is the outer part of the corona with a temperature lower than the average of the total corona. Thus, assume most of observed rapid variations take place at the joint region between the innermost disk and hot corona, the observed correlation character will be consistent with what is expected by the models mentioned above, and, in consequence, the average correlation coefficient of time segments with limited length will be a useful parameter to probe the corona geometry of X-ray binaries.

Another noticeable fact in our results is that the correlation coefficients r(h,f) on the 1 ms time scale listed in the third column of Table 1 are all negative, regardless what state Cyg X-1 was in. It is most probably an indication of the effect of Compton cooling of the local Comptonizing region by brief flashes. A considerable part of rapid variability of Cyg X-1 consists of many aperiodically occurring shots with widths distributed between  $\sim 30$  ms and  $\sim 0.2$  s (Feng, Li & Chen 1998). We used time segments of 10 ms duration to determine the correlation coefficients in the case of 1 ms time bin. In case of a 10 ms segment being contained by a shot, the average hardness in our correlation analysis reflects not the average temperature of total corona but that of local Comptonizing region of the shot. For this case a brief flashes of seed photons will decrease the local temperature and then the hardness of emitted x-rays.

Temporal structures on the time scale of 0.1 s in the high energy band are narrower than that in the low energy band as shown in Table 4, which is consistent with the average shot structures on the time scale  $\sim 0.1$  s in different energy bands obtained from PCA/RXTE observations of Cyg X-1 in different states (Feng, Li & Chen 1998), but contrary to the prediction of Comptonization models (Sunyaev & Titarchuk 1980, Hua, Kazanas & Cui 1997, Böttcher & Liang 1998a). This observed fact, together with the characteristic correlations between hardness and intensity revealed by our correlation analysis and shot analysis in the time domain, has to be considered in modeling the production process of X-rays from Cyg X-1. The hard X-ray time lag of Cyg X-1, expected by Comptonization process and revealed by Fourier frequency analysis is also shown in our results. It is interesting to see the time lags as a function of  $1/\Delta t$  (Fig.5) similar to that as a function of Fourier frequency (see, e.g., Nowak et al 1998, Fig.10). In comparison with the Fourier frequency, the time scale  $\Delta t$  is more directly related to the real physical processes causing

the rapid variabilities. At large time scales,  $\Delta t \geq 1$  s, average lags  $\overline{\lambda}$  change significantly with time, causing large  $\sigma_2$  in the last column of Table 5 and large error bars in the region of  $1/\Delta t \leq 1$  s<sup>-1</sup> in Figure 5. One can see from Fig.5 that the correlation analysis technique in the time domain we proposed has the capability to study the time lags at the short time scale region (or "high frequency" region  $1/\Delta t \geq 10$  s<sup>-1</sup>) with an enough precision. In this paper we use time lag bin  $\delta t = 1$  ms. A work of using higher time resolution data of RXTE to study time lags at the region  $1/\Delta t > 100$  s<sup>-1</sup> and correlations between hardness and intensity on time scales smaller than 1 ms is in the process, the results will be reported in a separate paper.

The authors thank Dr. Yu Weinfei for helpful discussions. We also thank the referee for valuable comments and suggestions. This research was supported by the National Natural Science Foundation of China and made use of data obtained through the High Energy Astrophysics Science Archive Research Center Online Service, provided by the NASA/Goddard Space Flight Center.

#### REFERENCES

Böttcher M. & Liang E.P. 1998a, astro-ph/9802283

Böttcher M. & Liang E.P. 1998b, ApJ submitted, (astro-ph/9810064)

Cui W., Heindl W.A., Rothschild R.E., Zhang S.N., Jahonda K. & Focke W. 1997a, ApJ, 474, L57

Cui W., Zhang S.N., Focke W. & Swank J.H. 1997b, ApJ, 484, 383

Dove J.B., Wilms J. & Begelman M.C. 1997, ApJ, 487, 747

Dove J.B., Wilms J., Maisack M.M. & Begelman M.C. 1997, ApJ, 487, 759

Eardley D.M., Lightman A.P. & Shapiro S. 1975, ApJ, 199, L153

Esin A.A., Narayan R., Cui W., Grove J.E. & Zhang S.N. 1998, ApJ in press, (astro-ph/9711167)

Feng Y.X., Li T.P. & Chen L. 1998, ApJ in press, (astro-ph/9810122)

Frank J., King A. & Raine D. 1992, Accretion Power in Astrophysics (Cambridge: Cambridge Univ. Press)

Haardt F. & Maraschi L. 1993, ApJ, 413, 507

Hua X.M., Kazanas D. & Cui W. 1997, Modeling the hard X-ray lag and energy spectrum of Cyg X-1, ApJ submitted, (astro-ph/9710184)

Hua X.M., Kazanas D.& Titarchuk L. 1997, ApJ, 482, L57

Kazanas D., Hua X.M. & Titarchuk L. 1997, ApJ, 480, 735

van der Klis, M. 1995, in X-Ray Binaries, ed. Lewin, W.H., van Paradijs, J., & van den Heuvel, E.P.J. (Cambridge: Cambridge Univ. Press)

Narayan R. & Yi I. 1994, ApJ, 428, L13

Narayan R., Mahadevan R. & Quataert E. 1998, in: The Theory of Black Accretion Discs, eds. M.A. Abramowicz, G. Bjornesson & J.E. Pringle, Cambridge Univ. Press, (astro-ph/9803141)

Negoro H., Miyamoto S. & Kitamoto S. 1994, ApJ, 423, L127

Nolan P.L., Gruber D.E., Matterson J.L., Peterson L.E., Rothschild R.E., Doty T.P., Levine A.M., Lewin W.H.G. & Primini F.A. 1981, ApJ, 246, 494

Nowak M.A., Vaughan B.A., Wilms J., Dove J.B. & Begelman C. 1998, ApJ in press, (astro-ph/9807278)

Nowak M.A., Wilms J., Vaughan B.A., Dove J.B., Mitchell C. & Begelman C. 1999, ApJ in press, (astro-ph/9810406)

Pottschmidt K., Koenig M., Wilms J. & Staubert R. 1998, A&A in press, (astro-ph/9802339)

Poutanen J. & Svensson R. 1996, ApJ, 470, 249

Priedhorsky W., Garmire G.P., Rothschild R.E., Boldt E., Serlemitsos P. & Holt S. 1979, ApJ, 233, 350

Sunyaev R.A. & Titarchuk L.G. 1980, A&A, 86, 121

Sutherland P.G, Weisskopf M.C. & Kahn S.M., 1978, ApJ, 219, 1029

Weisskopf M.C., Kahn S.M., & Sutherland P.G. 1975, ApJ, 199, L147

Weisskopf M.C., Sutherland P.G., Katz J.I. & Kahn S.M. 1978, ApJ, 223, L17

This preprint was prepared with the AAS IATEX macros v4.0.

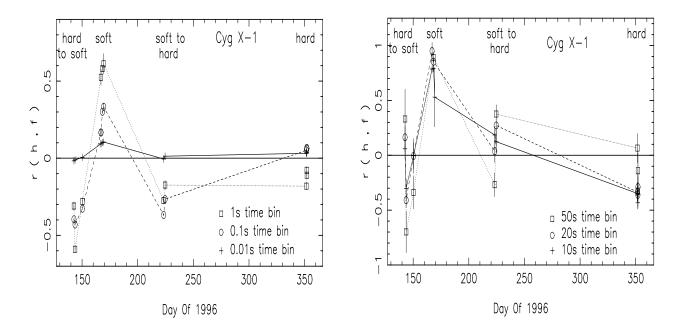


Fig. 1.— Correlation coefficients between hardness ratio h and intensity f(2-60 keV). For the periods of soft and transition states, h = f(13.1-60 keV)/f(2-6.5 keV). For the periods of hard states, h = f(13.1-60 keV)/f(2-5 keV). (a) in time bins 0.01 s, 0.1 s and 1 s; (b) in time bins 10 s, 20 s and 50 s.

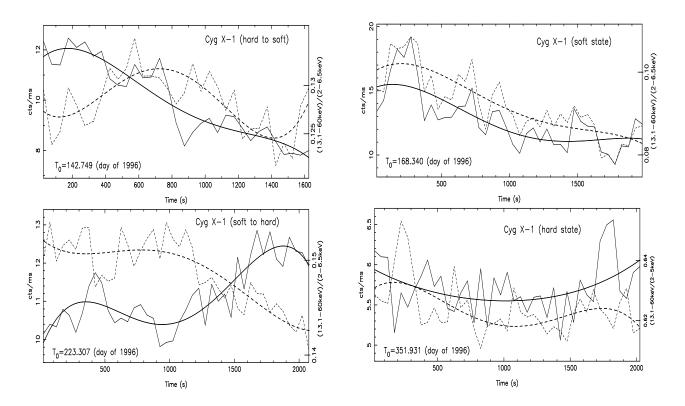


Fig. 2.— Intensity and hardness ratio profiles of four observation periods in different states. (a) Upper-left panel: hard-to-soft transition. (b) Upper-right panel: soft state. (c) Lower-left panel: soft-to-hard transition. (d) Lower-right panel: hard state. The solid fluctuated lines represent the light curve of 2–60 keV energy band in 50 s time bin, and the dotted fluctuated lines are the corresponding hardness ratio profiles of 13.1–60 keV and 2–6.5 keV (or 2–5 keV for the period of hard state). The solid and dotted smoothed lines are the least-squares fits of the intensity and hardness ratio distributions respectively.

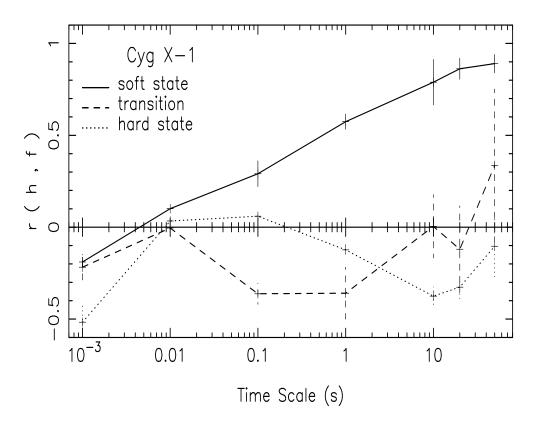


Fig. 3.— Correlation coefficient between hardness and intensity vs. time scale. Solid: soft state; Dashed: intermediate state; Dotted: hard state.

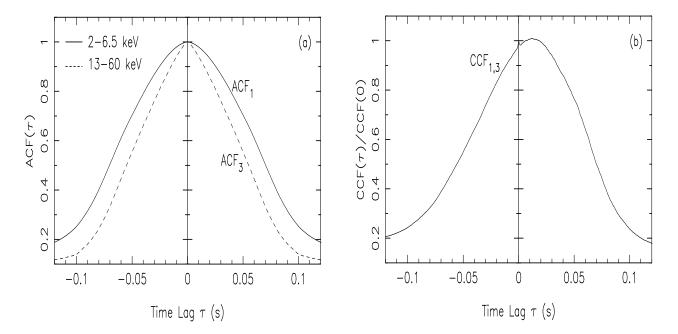


Fig. 4.— The average auto-correlation and cross-correlation functions of an observation period of Cyg X-1 in the transition from the hard state to the soft state. The observation started at 143.7 day of 1996. The time bin of light-curves  $\Delta t = 0.1$  s. (a) Left panel: the solid line is ACF of the low energy band (2–6.5 keV), the dashed line is ACF of the high energy band (13.1–60 keV). (b) Right panel: CCF between the low and high energy light-curves, normalized at the point  $\tau = 0$ .

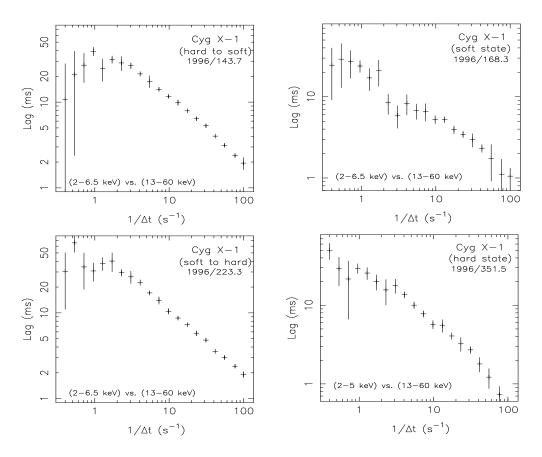


Fig. 5.— Hard X-ray lags between X-ray variations in the low energy and high energy bands of Cyg X-1 (2–5 keV vs. 13.1–60 keV for the hard state, 2–6.5 keV vs. 13.1–60 keV for the other states). The time lags are derived by the cross-correlation technique in the time domain for different time scales  $\Delta t$ . The error bars  $\sigma = \sqrt{\sigma_1^2 + \sigma_2^2}$ , where  $\sigma_1$  and  $\sigma_2$  are calculated by Eg.(8). (a) Upper-left panel: hard-to-soft transition. (b) Upper-right panel: soft state. (c) Lower-left panel: soft-to-hard transition. (d) Lower-right panel: hard state.

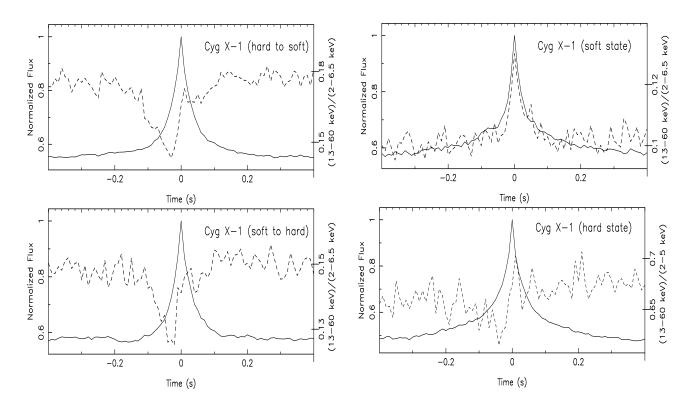


Fig. 6.— The intensity and hardness ratio profiles of average shots in different states of Cyg X-1. The solid lines are the superposed shot profiles with the peak height being normalized to be unity (from Fig.5 of Feng, Li & Chen 1998). The dashed lines are profiles of hardness ratio between the high and low energy band of average shots (from Fig.9 of Feng, Li & Chen 1998). (a) Upper-left panel: hard-to-soft transition. (b) Upper-right panel: soft state. (c) Lower-left panel: soft-to-hard transition. (d) Lower-right panel: hard state.

Table 1. Average Correlation Coefficients between Hardness and Intensity

| State      | Start Time    | Time Scale (s)     |                    |                    |                  |
|------------|---------------|--------------------|--------------------|--------------------|------------------|
| of Cyg X-1 | (Day of 1996) | $10^{-3}$          | $10^{-2}$          | $10^{-1}$          | 1                |
| Hard       | 142.7         | $-0.261 \pm 0.002$ | $-0.017 \pm 0.003$ | $-0.396 \pm 0.007$ | $-0.31 \pm 0.03$ |
| to         | 143.7         | $-0.194 \pm 0.001$ | $-0.011 \pm 0.002$ | $-0.430 \pm 0.007$ | $-0.59\pm0.02$   |
| Soft       | 150.3         | $-0.349 \pm 0.005$ | $0.006\pm0.003$    | $-0.327 \pm 0.007$ | $-0.28\pm0.03$   |
|            | 167.0         | $-0.235 \pm 0.008$ | $0.094 \pm 0.008$  | $0.17 \pm 0.02$    | $0.52 \pm 0.05$  |
| Soft       | 168.3         | $-0.189 \pm 0.002$ | $0.101\pm0.002$    | $0.301\pm0.007$    | $0.58 \pm 0.02$  |
|            | 169.3         | $-0.174 \pm 0.005$ | $0.105\pm0.008$    | $0.33 \pm 0.02$    | $0.61 \pm 0.07$  |
| Soft to    | 223.3         | $-0.222 \pm 0.001$ | $-0.005 \pm 0.003$ | $-0.368 \pm 0.006$ | $-0.27 \pm 0.02$ |
| Hard       | 224.6         | $-0.371 \pm 0.007$ | $0.013\pm0.003$    | $-0.265 \pm 0.008$ | $-0.17\pm0.03$   |
|            | 351.5         | $-0.392 \pm 0.002$ | $0.032 \pm 0.002$  | $0.051 \pm 0.007$  | $-0.18 \pm 0.02$ |
| Hard       | 351.9         | $-0.546 \pm 0.002$ | $0.036\pm0.002$    | $0.067\pm0.008$    | $-0.08\pm0.02$   |
|            | 352.0         | $-0.613 \pm 0.002$ | $0.033 \pm 0.002$  | $0.062 \pm 0.006$  | $-0.11 \pm 0.02$ |

Table 2. Average Correlation Coefficients between Hardness and Intensity

| State      | Start Time    |                  | Time Scale (s)   |                  |
|------------|---------------|------------------|------------------|------------------|
| of Cyg X-1 | (Day of 1996) | 10               | 20               | 50               |
| Hard       | 142.7         | $0.06 \pm 0.09$  | $0.16 \pm 0.10$  | $0.33 \pm 0.27$  |
| to         | 143.7         | $-0.30 \pm 0.08$ | $-0.41\pm0.07$   | $-0.70\pm0.19$   |
| Soft       | 150.3         | $-0.01 \pm 0.12$ | $-0.01\pm0.16$   | $-0.34\pm0.15$   |
|            | 167.0         | $0.79 \pm 0.02$  | $0.95 \pm 0.08$  |                  |
| Soft       | 168.3         | $0.79 \pm 0.03$  | $0.85 \pm 0.03$  | $0.89 \pm 0.05$  |
|            | 169.3         | $0.53 \pm 0.27$  |                  |                  |
| Soft to    | 223.3         | $0.18 \pm 0.08$  | $0.04 \pm 0.10$  | $-0.27 \pm 0.11$ |
| Hard       | 224.6         | $0.12 \pm 0.09$  | $0.27 \pm 0.19$  | $0.38 \pm 0.02$  |
|            | 351.5         | $-0.35 \pm 0.07$ | $-0.34 \pm 0.09$ | $0.07 \pm 0.13$  |
| Hard       | 351.9         | $-0.43 \pm 0.06$ | $-0.36\pm0.11$   | $-0.33\pm0.16$   |
|            | 352.0         | $-0.35 \pm 0.05$ | $-0.29\pm0.09$   | $-0.14\pm0.16$   |

Table 3. FWHM of ACF of Low Energy Photons

| State      | Start Time    |                             | $\mathrm{FWHM}_1/\Delta t$ | _                        |
|------------|---------------|-----------------------------|----------------------------|--------------------------|
| of Cyg X-1 | (Day of 1996) | $\Delta t = 0.01 \text{ s}$ | $\Delta t = 0.1 \text{ s}$ | $\Delta t = 1 \text{ s}$ |
| Soft       | 168.3         | $0.410 \pm 0.002 \pm 0.012$ | $1.63 \pm 0.01 \pm 0.05$   | $1.25 \pm 0.05 \pm 0.15$ |
| State      | 169.3         | $0.469 \pm 0.002 \pm 0.007$ | $1.47 \pm 0.02 \pm 0.05$   | $1.08 \pm 0.07 \pm 0.13$ |
| Transition | 143.7         | $0.548 \pm 0.002 \pm 0.012$ | $1.58 \pm 0.01 \pm 0.04$   | $0.71 \pm 0.02 \pm 0.09$ |
| State      | 223.3         | $0.503 \pm 0.002 \pm 0.007$ | $1.42 \pm 0.01 \pm 0.04$   | $0.77 \pm 0.04 \pm 0.18$ |
| Hard       | 351.5         | $0.674 \pm 0.003 \pm 0.011$ | $1.63 \pm 0.01 \pm 0.04$   | $1.41 \pm 0.05 \pm 0.14$ |
| State      | 351.9         | $0.691 \pm 0.003 \pm 0.013$ | $1.63 \pm 0.01 \pm 0.05$   | $1.31 \pm 0.05 \pm 0.17$ |

Table 4. ACF Width Ratio of High Energy Photons to Low Energy Photons

| State      | Start Time    | $FWHM_3/FWHM_1$             |                             |                          |
|------------|---------------|-----------------------------|-----------------------------|--------------------------|
| of Cyg X-1 | (Day of 1996) | $\Delta t = 0.01 \text{ s}$ | $\Delta t = 0.1 \text{ s}$  | $\Delta t = 1 \text{ s}$ |
| Soft       | 168.3         | $2.09 \pm 0.01 \pm 0.11$    | $0.87 \pm 0.01 \pm 0.05$    | $1.11 \pm 0.07 \pm 0.12$ |
| State      | 169.3         | $2.15 \pm 0.01 \pm 0.06$    | $0.75 \pm 0.01 \pm 0.05$    | $0.91 \pm 0.07 \pm 0.16$ |
| Transition | 143.7         | $1.440 \pm 0.008 \pm 0.019$ | $0.747 \pm 0.009 \pm 0.016$ | $0.87 \pm 0.05 \pm 0.19$ |
| State      | 223.3         | $1.580 \pm 0.009 \pm 0.015$ | $0.785 \pm 0.009 \pm 0.021$ | $1.05 \pm 0.08 \pm 0.24$ |
| Hard       | 351.5         | $1.194 \pm 0.006 \pm 0.022$ | $0.94 \pm 0.01 \pm 0.03$    | $0.97 \pm 0.05 \pm 0.10$ |
| State      | 351.9         | $1.173 \pm 0.007 \pm 0.014$ | $0.95 \pm 0.01 \pm 0.03$    | $0.97 \pm 0.05 \pm 0.14$ |

Table 5. Time Delay of High Energy Photons to Low Energy Photons

| State      | Start Time    | Time Delay (ms)             |                            |                          |
|------------|---------------|-----------------------------|----------------------------|--------------------------|
| of Cyg X-1 | (Day of 1996) | $\Delta t = 0.01 \text{ s}$ | $\Delta t = 0.1 \text{ s}$ | $\Delta t = 1 \text{ s}$ |
| Soft       | 168.3         | $0.700 \pm 0.005 \pm 0.024$ | $17.1 \pm 0.5 \pm 1.8$     | $28.3 \pm 2.2 \pm 9.2$   |
| State      | 169.3         | $0.817 \pm 0.009 \pm 0.047$ | $24.0 \pm 0.8 \pm 1.6$     | $37.9 \pm 5.0 \pm 52.3$  |
| Transition | 143.7         | $0.696 \pm 0.004 \pm 0.015$ | $23.3 \pm 0.5 \pm 1.7$     | $23.2 \pm 2.3 \pm 24.2$  |
| State      | 223.3         | $0.688 \pm 0.004 \pm 0.009$ | $23.1 \pm 0.4 \pm 1.4$     | $32.1 \pm 2.7 \pm 14.0$  |
| Hard       | 351.5         | $0.749 \pm 0.006 \pm 0.014$ | $16.4 \pm 0.4 \pm 0.8$     | $22.1 \pm 1.9 \pm 5.5$   |
| State      | 351.9         | $0.751 \pm 0.006 \pm 0.016$ | $16.2 \pm 0.4 \pm 1.5$     | $22.3 \pm 2.2 \pm 7.4$   |